Blood and Lymphatic Cancer: Targets and Therapy

Dovepress
Taylor & Francis Group

Open Access Full Text Article

ORIGINAL RESEARCH

Short-Term Longitudinal Analysis of Gut Microbiota Dynamics During Anti-CD19 CAR-T Cell Therapy in Diffuse Large B-Cell Lymphoma Patients

Ziyuan Shen[1], Xing Xing[2], Kang Rong[3], Ziyang Geng[4], Ning Yang[5], Linyan Xu[3,6], Hongfeng Ge[7], Wei Sang[3,6,8]

[1]Clinical Research Institute, the Affiliated Hospital of Xuzhou Medical University, Xuzhou, Jiangsu, People's Republic of China; [2]Department of Biostatistics, Johns Hopkins Bloomberg School of Public Health, Baltimore, Maryland, USA; [3]Department of Hematology, The Affiliated Hospital of Xuzhou Medical University, Xuzhou, Jiangsu, People's Republic of China; [4]The Second Clinical Medical College, Xuzhou Medical University, Xuzhou, Jiangsu, People's Republic of China; [5]Department of Gastroenterology, The First People's Hospital of Xuzhou, Xuzhou, Jiangsu, People's Republic of China; [6]Blood Diseases Institute, Xuzhou Medical University, Xuzhou, Jiangsu, People's Republic of China; [7]Department of Hematology, Bozhou People's Hospital, Bozhou, Anhui, People's Republic of China; [8]Cell Research and Translational Medicine Center, The Affiliated Hospital of Xuzhou Medical University, Xuzhou, Jiangsu, People's Republic of China

Correspondence: Wei Sang, Department of Hematology, The Affiliated Hospital of Xuzhou Medical University, Xuzhou, Jiangsu, People's Republic of China, Email xyfylbl515@xzhmu.edu.cn; Hongfeng Ge, Department of Hematology, Bozhou People's Hospital, Bozhou, Anhui, People's Republic of China, Email ghfzz@163.com

Purpose: Alterations in gut microbiota may influence immune response and treatment outcomes in patients with diffuse large B-cell lymphoma (DLBCL). However, the dynamics during anti-CD19 CAR-T cell therapy remain unclear.

Methods: We conducted a short-term longitudinal microbiome analysis in DLBCL patients (n=12) undergoing CAR-T cell therapy targeting CD19. Stool samples were collected at baseline, 1 week, and 2 weeks post-infusion. 16S rRNA gene sequencing was used to assess microbial diversity, taxonomic composition, and functional pathways. Correlation analyses were then conducted between microbial taxa and inflammatory biomarkers.

Results: Alpha diversity indices showed no statistically significant differences across time points. Beta diversity analysis revealed distinct clustering between baseline and week 1 samples in sPLS-DA, although PERMANOVA did not reach statistical significance. At the phylum level, Bacteroidota abundance significantly increased at week 2 compared with baseline (P = 0.008), accompanied by a marked reduction in the Firmicutes/Bacteroidota ratio. Genus-level heatmap and LEfSe analysis identified enrichment of *Parabacteroides*, and *Prevotella* at week 2, whereas baseline samples were enriched in Clostridium sensu stricto 13 and *Fusobacterium*. Functional prediction indicated that lipoic acid metabolism pathways were significantly upregulated at weeks 1 and 2 compared with baseline (both $P < 0.05$). Correlation analysis demonstrated that specific bacterial taxa, including *Parabacteroides* and *Prevotella*, were positively associated with lymphocyte counts and inversely correlated with C-reactive protein levels.

Conclusion: Gut microbiota alterations following CAR-T infusion, characterized by increased Bacteroidota abundance, specific taxonomic shifts, and enhanced lipoic acid metabolism, may provide early microbial signatures for monitoring immune modulation in DLBCL patients.

Keywords: anti–CD19 CAR–T, diffuse large B–cell lymphoma, microbiome dynamics

Introduction

Diffuse large B-cell lymphoma (DLBCL) is the most common subtype of non-Hodgkin lymphoma, characterized by biological and clinical heterogeneity.[1] While frontline immunochemotherapy regimens have significantly improved survival outcomes, a substantial proportion of patients ultimately relapse or develop refractory disease.[2,3] Chimeric antigen receptor T (CAR-T) cell therapy has emerged as a promising treatment option for relapsed or refractory DLBCL,

https://doi.org/10.2147/BLCTT.S598958
Received: 14 February 2026
Accepted: 24 April 2026
Published: 1 May 2026

offering durable responses in a subset of patients.[4] However, the treatment is often accompanied by serious complications such as cytokine release syndrome, the mechanisms of which remain incompletely understood.[5,6]

Recent evidence suggests that the gut microbiota plays a crucial role in modulating host immune responses and influencing the efficacy and toxicity of cancer immunotherapies, particularly immune checkpoint inhibitors.[7,8] The gut microbiome may serve as a key mediator linking systemic immunity with therapeutic outcomes. Diefenbach et al reported that pretreatment gut microbial composition and diversity differed significantly between indolent lymphomas and aggressive subtypes such as DLBCL.[9] A study of untreated DLBCL patients revealed distinct gut microbial alterations compared to healthy controls, including reduced beta-diversity and imbalances in key bacterial phyla.[10] These findings highlight the intrinsic connection between gut microbiota and lymphoma biology.

While previous studies have primarily focused on the predictive value of pretreatment gut microbiota for CAR-T therapy outcomes,[5,11] our study targeted patients who achieved confirmed clinical responses. CAR-T cell therapy is known to induce robust immune activation and systemic inflammation; however, it remains unclear whether these responses are accompanied by dynamic alterations in the gut microbiota. In this study, we conducted a longitudinal analysis of 12 DLBCL patients who responded to anti-CD19 CAR-T therapy (complete or partial response) and had fecal samples available at three clinically relevant time points: pre-infusion, and at weeks 1 and 2 post-infusion. This design enabled us to capture microbiota dynamics during the acute post-infusion phase and explore their potential associations with systemic inflammatory and immune parameters, providing new insights into microbiota-immune crosstalk in the setting of effective CAR-T treatment.

Materials and Methods

Study Design and Patients

In this study, all patients with DLBCL were recruited from the Affiliated Hospital of Xuzhou Medical University between September 2023 and May 2024. Patients with a history of gastrointestinal surgery or active gastrointestinal diseases, recent use of oral antibiotics, probiotics, or bowel-cleansing agents (within 4 weeks prior to sampling), coexisting active malignancies, or serious immunodeficiency or autoimmune disorders were excluded. Clinical data, including age, gender, lymphocyte count, serum albumin, neutrophil count, white blood cell count, C-reactive protein (CRP) level, and Eastern Cooperative Oncology Group performance status (ECOG PS), were collected.

All patients received the same anti-CD19 CAR-T product, a second-generation CAR-T therapy incorporating a 4–1BB costimulatory domain, manufactured by Aikangde Biotechnology Co., Ltd. (Suzhou, China). The infused dose ranged from 1.8 to 4.6×10^6 CAR-T cells/kg [median dose: 2.1×10^6 CAR-T cells/kg]. Regarding treatment-related toxicities, grade 1 cytokine release syndrome (CRS) occurred in 5 patients and grade 2 CRS occurred in 2 patients. No immune effector cell-associated neurotoxicity syndrome was observed.

Stool Sample Collection and Time Points

Stool samples were collected at three time points: prior to CAR-T cell infusion (baseline), one week after infusion, and two weeks after infusion. All samples were collected using sterile collection kits containing a preservation solution. Participants were instructed to collect stool directly onto clean, dry toilet paper, avoiding contact with other bodily fluids. Approximately 200 mg of stool was sampled from the middle portion using a sterile swab and immediately immersed in the preservation solution. The swab was discarded after ensuring adequate mixing of the sample with the solution by shaking for 30–60 s. Samples were sealed in individual, light-proof bags, labeled with unique identifiers, stored at 4°C, and transported to the laboratory within 24 h for downstream 16S rRNA gene sequencing analysis to systematically evaluate gut microbiome dynamics across different stages of CAR-T therapy.

DNA Extraction and Sequencing

Upon completion of sequencing, demultiplexing of the obtained reads was performed using an in-house bioinformatics script. All downstream analyses were conducted using the Quantitative Insights Into Microbial Ecology 2 (QIIME2, version 2021.11) platform.[12] The DADA2 pipeline[13] was applied for paired-end read merging, quality filtering, chimera

removal, and denoising, followed by clustering of high-quality sequences into amplicon sequence variants (ASVs). Taxonomic assignment of these features was performed against the SILVA database (release 132) using QIIME2's classify-sklearn classifier, and a feature table was generated.

Bioinformatics and Data Analysis

Alpha diversity was assessed using multiple indices, including ACE, Chao1, observed species, PD_whole_tree, Shannon, Simpson, and Goods_coverage. Beta diversity was calculated based on Bray-Curtis distances and visualized by principal coordinate analysis (PCoA) and sparse partial least squares discriminant analysis (sPLS-DA). Permutational multivariate analysis of variance (PERMANOVA) was performed using the adonis function in the vegan R package to evaluate differences in microbial community structure across time points. Stage-dependent features were identified using linear discriminant analysis effect size (LEfSe) with a logarithmic LDA score threshold of 2.5.[14]

Microbial functional prediction was conducted using PICRUSt2[15] based on ASVs clustered from the 16S rRNA sequencing data, and functional annotations were mapped to the Kyoto Encyclopedia of Genes and Genomes (KEGG) database.[16] Differences in predicted pathways between time points were analyzed using Welch's *t*-test, with multiple testing correction performed using the Benjamini-Hochberg false discovery rate (FDR) method in STAMP (version 2.1.3).[17]

Statistical Analysis

As this was an exploratory longitudinal microbiome study, no formal a priori sample size calculation was performed. The sample size was determined by the number of eligible patients with DLBCL who underwent anti-CD19 CAR-T therapy and had longitudinal fecal samples available during the study period. Given the limited prior effect size estimates for short-term gut microbiota changes in this clinical setting, the present study was intended to generate preliminary data for future validation in larger cohorts.

Longitudinal comparisons of the Chao1 index and selected microbial taxa were performed using linear mixed-effects models, with time point included as a fixed effect and subject ID included as a random effect to account for within-subject correlation due to repeated measurements. Models were fitted using restricted maximum likelihood (REML), and a two-sided P value < 0.05 was considered statistically significant.

Pearson's correlation analysis was used as an exploratory analysis to assess associations between microbial taxa and inflammatory markers, including lymphocyte count, serum albumin, neutrophil count, white blood cell count, and CRP. A two-sided P value < 0.05 was considered statistically significant unless otherwise specified.

Results

Baseline Characteristics of DLBCL Patients

All patients achieved a clinical response and had longitudinally available fecal samples for microbiome profiling. Among them, 8 (66.7%) achieved a complete response and 4 achieved a partial response following CAR-T cell infusion. The median age of the 12 patients was 54 years, and 58.3% (n = 7) were male. The median LDH level was 202 U/L. According to ECOG PS, 41.7% (n = 5) of patients had a score < 2, while 58.3% (n = 7) had a score ≥ 2. At a median follow-up of 20.4 months, the estimated 1-year overall survival (OS) rate was 83.3%.

α- and β-Diversity Analysis Across Time Points

α-diversity analysis showed that overall microbial richness and diversity exhibited a slight upward trend over time (Figure 1A–G). Richness-related indices, including Chao1, ACE, and observed OTUs, increased slightly at week 2 after treatment, although the differences were not statistically significant. To account for within-subject correlations arising from repeated sampling, linear mixed-effects modeling was further performed and confirmed that the Chao1 index did not differ significantly across time points. The PD_whole_tree index also showed a mild increase at week 2, suggesting a slight enhancement in phylogenetic diversity. The Shannon index increased slightly, whereas the Simpson index decreased marginally at week 2, indicating a trend toward higher diversity and evenness. Good's coverage values were consistently close to 1 (~99.99%) across all time points, indicating adequate sequencing depth to capture the majority of

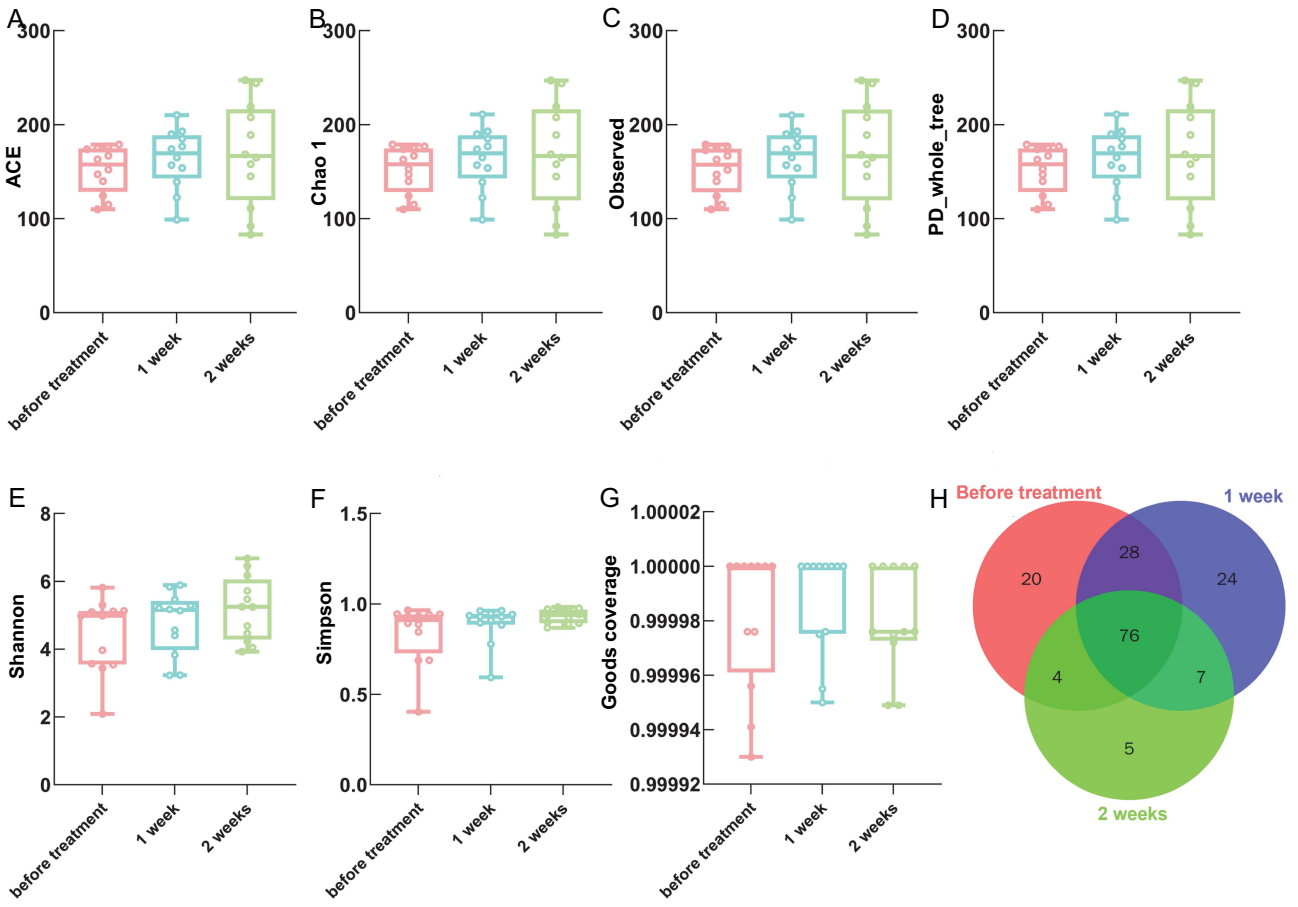

Figure 1 Alpha diversity analysis of gut microbiota. (**A**–**G**) Various α-diversity indices were used to assess microbial diversity across treatment groups. (**H**) Venn diagram illustrating the shared and unique differential microbiota among the different treatment groups.

taxa present. The Venn diagram (Figure 1H) showed that 76 OTUs were detected at all three time points. Notably, week 1 after treatment had the highest number of unique OTUs (n=24), suggesting that CAR-T therapy may cause short-term perturbations in gut microbiota composition, with partial recovery observed by week 2.

β-diversity was evaluated using PCoA based on Bray-Curtis distances (Figure 2A). The three groups showed a partial separation along the PC1 and PC2 axes; however, PERMANOVA analysis indicated no statistically significant differences (R^2 = 0.0681, P = 0.122). Pairwise comparisons of Bray-Curtis distances revealed that the most pronounced difference occurred between baseline and week 2 ($P < 0.05$).

The sPLS-DA analysis further demonstrated distinct clustering and separation among the three groups (Figure 2B). Notably, samples collected at week 1 exhibited the tightest clustering and were most clearly separated from both baseline and week 2, suggesting a marked shift in microbial composition at this time point. By week 2, the distribution of samples appeared more similar to baseline, indicating a partial recovery following the initial perturbation.

Temporal Changes in Microbiome Composition Following CAR-T Therapy

At the phylum level (Figure 3A), Firmicutes, Bacteroidota, and Proteobacteria were the dominant taxa across all time points. Linear mixed-effects modeling showed that the relative abundance of Bacteroidota was significantly lower at week 1 than at week 2 (P = 0.002), whereas the difference between baseline and week 2 did not reach statistical significance (P = 0.113). Firmicutes showed a decreasing trend over time (Figure 3D), resulting in a reduced Firmicutes/Bacteroidota (F/B) ratio (Figure 3F). The heatmap (Figure 3C) revealed distinct clustering patterns among the three time points. Compared with baseline, samples from weeks 1 and 2 post-treatment showed a reduced relative abundance of certain opportunistic pathogens, such as *Escherichia-Shigella* and *Enterococcus*, along with an increased relative

 https://doi.org/10.2147/BLCTT.S598958

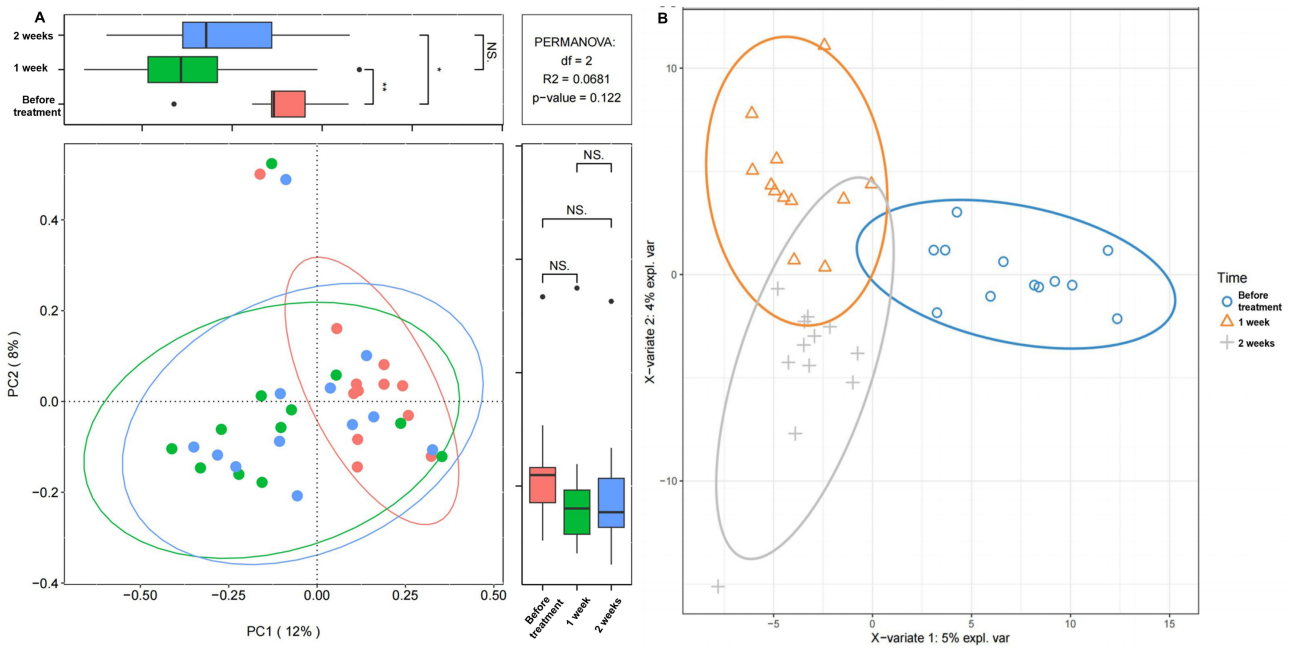

Figure 2 Beta diversity analysis of gut microbiota. (**A**) Principal Coordinates Analysis (PCoA) based on gut microbiota composition. (**B**) Sparse partial least squares discriminant analysis (sPLS-DA) illustrating group separation based on microbial community structure. *$P < 0.05$; **$P < 0.01$.
Abbreviation: NS, not significant.

abundance of genera commonly associated with gut health, including *Faecalibacterium, Lachnospira*, and *Bacteroides*. By week 2, the overall community composition appeared more similar to baseline, although some characteristic shifts persisted, suggesting that the impact of CAR-T therapy on gut microbiota is short-term and partially reversible.

Further analysis showed that Proteobacteria abundance was significantly elevated at week 1 post-treatment ($P = 0.048$, Supplementary Figure 1A), whereas *Enterococcus* showed a slight increase at week 1 followed by a decrease at week 2 (Supplementary Figure 1B).

Differentially Enriched Taxa Across Treatment Time Points

LEfSe analysis identified taxa that were significantly enriched at different time points, as shown in the LDA score bar plot (Figure 4A). At baseline, enriched taxa included Coriobacteriales, *Fusobacterium mortiferum*, and *Clostridium leptum*. At week 1 post-treatment, the dominant enriched taxa were *Enterococcus, Klebsiella*, and *Lactobacillus*, along with multiple members of the families Veillonellaceae, Desulfovibrionaceae, and Peptostreptococcaceae. Several potentially opportunistic taxa, including Enterobacteriaceae within the phylum Proteobacteria, were also enriched at this time point. By week 2 post-treatment, significantly enriched taxa included Prevotellaceae, *Parabacteroides, Prevotella*, Faecalibacterium, and several health-associated taxa such as Tannerellaceae and Barnesiellaceae. The cladogram illustrated that these differential taxa clustered across multiple taxonomic levels from phylum to genus, indicating a time-dependent restructuring of the microbial community following CAR-T cell therapy (Figure 4B).

Altered Microbial Functions and Correlations with Inflammatory Indicators

Functional prediction analysis (Figure 5A) showed that the relative abundance of the lipoic acid metabolism pathway was significantly higher at both week 1 and week 2 post-treatment compared with baseline, with P values <0.02 and <0.05, respectively.

Correlation analysis (Figure 5B) revealed significant associations between multiple clinical parameters and differential bacterial genera. CRP was positively correlated with *Enterococcus, Escherichia-Shigella*, and *Streptococcus*, and negatively correlated with *Faecalibacterium* and *Bifidobacterium*. WBC and neutrophil count were positively associated with potentially pathogenic taxa such as *Enterococcus* and *Escherichia-Shigella*, whereas lymphocyte count was

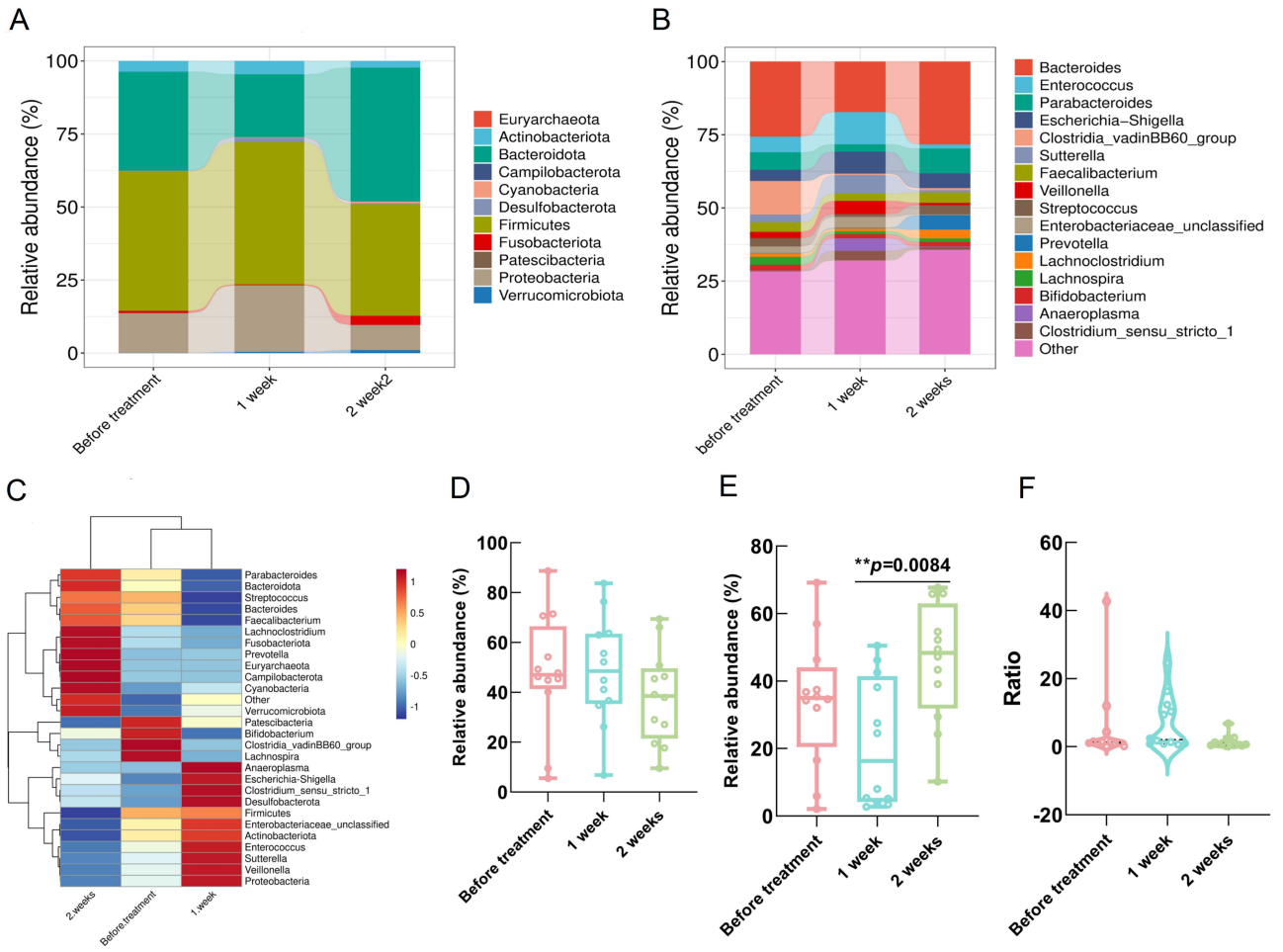

Figure 3 Comparison of gut microbiota abundance across different time points. (**A**) Relative abundance of dominant gut microbiota at the phylum level. (**B**) Relative abundance of dominant gut microbiota at the genus level. (**C**) Heatmap showing hierarchical clustering of gut microbiota at both phylum and genus levels. (**D**) Relative abundance of Firmicutes across treatment groups. (**E**) Relative abundance of Bacteroidota across treatment groups. (**F**) Ratio of Firmicutes to Bacteroidota across treatment groups. *$P < 0.05$; **$P < 0.01$.
Abbreviation: NS, not significant.

positively correlated with *Faecalibacterium*. Albumin levels showed positive correlations with health-associated genera, including *Bacteroides* and *Faecalibacterium*, and negative correlations with certain potentially harmful bacteria.

Discussion

In this longitudinal study, we focused on a subset of DLBCL patients who achieved clear clinical responses to CAR-T therapy and profiled their gut microbiota at three early post-infusion time points. We observed subtle and transient changes in microbial community composition, including a trend toward enrichment of health-associated taxa and a reduction in opportunistic pathogens, as well as functional changes inferred from predictive analysis, notably involving lipoic acid metabolism. These findings provide preliminary insight into short-term microbiome dynamics during the early phase after CAR-T infusion and suggest that microbial profiles, combined with host inflammatory markers, may be related to host immune status and treatment-associated inflammation.

In this study, although α diversity metrics did not change significantly, the transient separation of week 1 samples from baseline in sPLS-DA suggested limited temporal variation in intestinal microbial composition during the peak immune activation phase following CAR-T infusion. Given that the overall beta diversity separation was modest, this finding should be interpreted cautiously as a preliminary compositional fluctuation rather than distinct microbiome restructuring. Similar phenomena have been reported in patients receiving immune checkpoint inhibitor therapy.

https://doi.org/10.2147/BLCTT.S598958

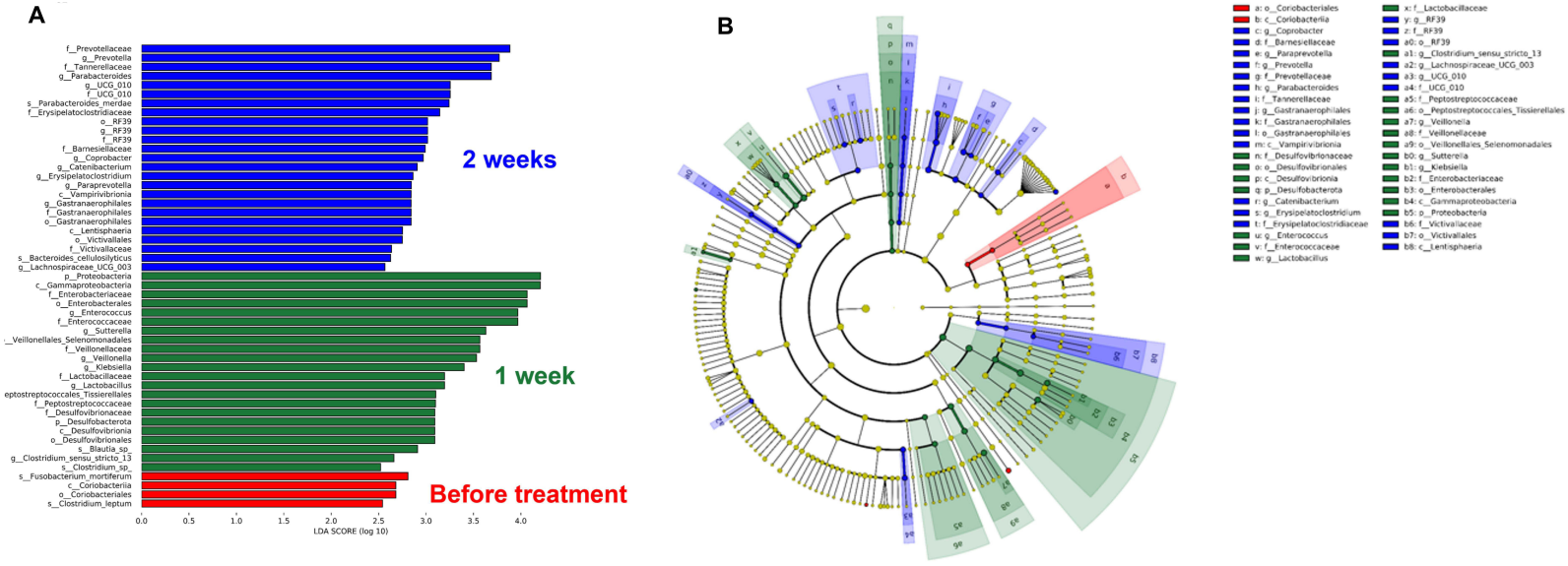

Figure 4 Linear discriminant analysis effect size (LEfSe) of gut microbiota. (**A**) Bar plot of significantly different taxa identified by LEfSe among treatment groups, based on LDA scores. (**B**) Cladogram illustrating the phylogenetic distribution of differentially abundant taxa identified by LEfSe.

https://doi.org/10.2147/BLCTT.S598958

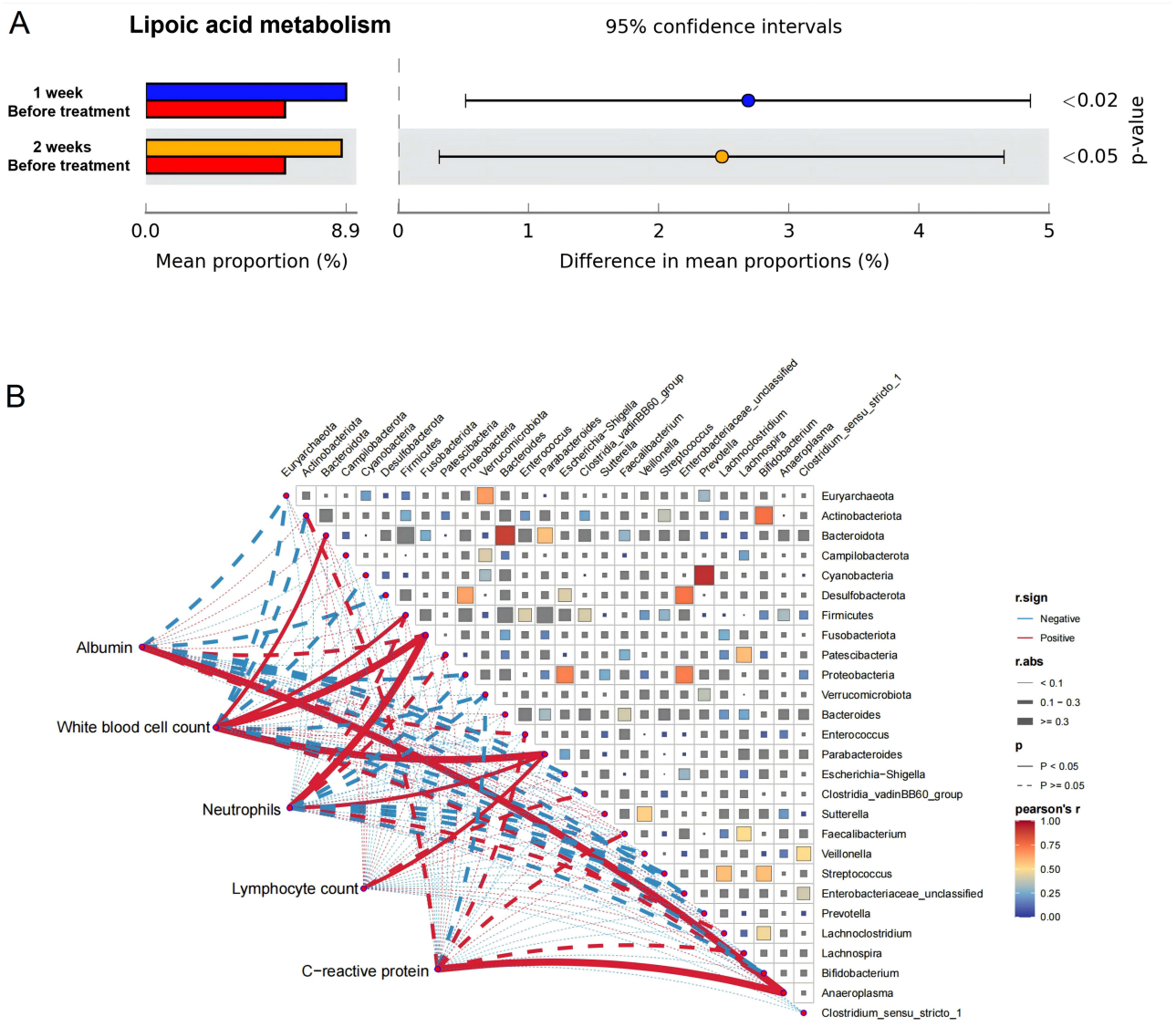

Figure 5 Functional prediction and correlation analysis of gut microbiota. (**A**) Functional prediction of gut microbiota. (**B**) Correlation analysis of microbial taxa, illustrating relationships among dominant genera.

A previous study demonstrated that in patients with hematologic malignancies treated with anti-CD19 CAR-T cells, reduced gut microbiota diversity was associated with immune-related toxicities and was accompanied by significant enrichment of *Enterococcus* and *Actinomyces*.[18] In a longitudinal cohort of patients with multiple myeloma, greater post-treatment disruption of the gut microbiota was also linked to increased toxicity.[19] Consistent with these findings, we observed partial reversion of the microbial community toward baseline by week 2, suggesting that such alterations may be transient and partially reversible. Potential mechanisms include inflammation induced by CAR-T-associated cytokine release, alterations in intestinal mucosal permeability, and changes in antimicrobial peptide secretion patterns, all of which have been reported in experimental models of acute inflammation.[20–23]

At the phylum level, the increase in the relative abundance of Bacteroidota at week 2, accompanied by a reduction in the F/B ratio, may be of interest, as similar microbial patterns have been associated with improved metabolic status and reduced inflammatory levels in other immunotherapy settings.[24,25] In a study of melanoma patients treated with immune checkpoint inhibitors, responders exhibited significantly higher Bacteroidota abundance and a lower F/B ratio compared

https://doi.org/10.2147/BLCTT.S598958

with non-responders.[8] This microbial profile was associated with higher levels of short-chain fatty acids production, improved intestinal barrier function, and lower levels of pro-inflammatory cytokines, which are thought to enhance antitumor immune responses and mitigate treatment-related inflammation.[26] Importantly, the F/B ratio has long been regarded as an ecological marker of intestinal and systemic homeostasis. A lower F/B ratio has been linked to reduced endotoxemia, improved metabolic flexibility, and favorable immunotherapy responses in both solid and hematologic malignancies.[27,28] At the genus level, the enrichment of *Faecalibacterium, Lachnospira*, and *Bacteroides* is consistent with their known anti-inflammatory properties, including short-chain fatty acid production and maintenance of epithelial barrier integrity. In contrast, the enrichment at week 1 of *Enterococcus, Klebsiella*, and members of the family Veillonellaceae, many of which have been linked to bloodstream infections and adverse immunotherapy outcomes, may reflect transient dysbiosis during the early phase after CAR-T infusion.[5]

LEfSe analysis identified taxa that were differentially enriched across time points following CAR-T infusion, with several opportunistic and potentially pro-inflammatory taxa enriched at week 1 and several commensal and potentially beneficial taxa enriched at week 2. This pattern may be consistent with a transient perturbation followed by partial recovery.[29,30] Similar transient post-treatment microbial shifts have been reported in other immunotherapy settings. Subsequent recovery of beneficial taxa, particularly butyrate producers, has been linked to restoration of immune homeostasis and attenuation of inflammation.[8,31] The enrichment of Prevotellaceae, *Parabacteroides*, and *Faecalibacterium* at week 2 may indicate partial microbial recovery. These taxa are well-recognized producers of short-chain fatty acids, which can enhance mucosal barrier integrity and downregulate pro-inflammatory signaling pathways,[32] thereby facilitating immune reconstitution and inflammation control.

Functional prediction analysis based on 16S rRNA sequencing suggested potential enrichment of lipoic acid metabolism following CAR-T cell infusion. Lipoic acid is a critical mitochondrial cofactor involved in energy metabolism and redox regulation, with potent antioxidant properties that enable scavenging of reactive oxygen species, regeneration of other antioxidants such as glutathione, and preservation of mitochondrial function.[33–35] However, this pathway-level enrichment was inferred from predictive bioinformatic analysis rather than measured directly, and should therefore be interpreted cautiously. Moreover, our correlation analysis showed that health-associated taxa enriched in short-chain fatty acid production, such as *Faecalibacterium* and *Bacteroides*, were positively correlated with lymphocyte counts and serum albumin levels, whereas opportunistic taxa including *Enterococcus* and *Escherichia-Shigella* were positively correlated with CRP, WBC counts, and neutrophil counts.

This study characterized short-term compositional changes and predicted functional shifts in the gut microbiota of patients with DLBCL undergoing CAR-T therapy through repeated sampling and correlation analyses with inflammatory and immune parameters. Although the observed differences were relatively subtle, they provide preliminary evidence that the gut microbiota may undergo early alterations during the acute post-infusion phase. Several limitations should be acknowledged. First, the small cohort size (n = 12) and single-center design limit the statistical power, robustness, and generalizability of the findings. Second, although the longitudinal repeated-sampling design partially reduced inter-individual heterogeneity, gut microbiota composition during CAR-T treatment may still have been influenced by concurrent factors such as antibiotic exposure, dietary changes, hospitalization-related conditions, and lymphodepletion chemotherapy. Third, the use of 16S rRNA sequencing limits taxonomic resolution and the reliability of functional inference, and the predicted functional findings should therefore be interpreted with caution. Accordingly, the present results should be considered exploratory and preliminary. Overall, the observed microbial changes may indicate a potential link between gut microbiota dynamics and host immune status during CAR-T treatment. Larger multicenter studies with longer follow-up and multi-omics approaches are needed to validate these findings and further clarify the interaction between the gut microbiota and host immunity during CAR-T therapy.

Data Sharing Statement

The datasets generated and/or analyzed during the current study are available from the corresponding author (Dr. Wei Sang, xyfylbl515@xzhmu.edu.cn) upon reasonable request.

Ethics Approval and Consent to Participate

This study was conducted in accordance with the ethical principles of the Declaration of Helsinki, and study approval was obtained from the ethics committee of the Affiliated Hospital of Xuzhou Medical University (XYFY2022-KL480-02). Informed consent was obtained from each patient.

Acknowledgments

We sincerely thank Dr. Lei Yu from Xuzhou Kang Shiyou Institute of Health and Medical Technology Co., Ltd. for his valuable support in data acquisition and sequencing services for this study.

Author Contributions

Ziyuan Shen, Xing Xing, and Kang Rong are joint first authors. All authors made a significant contribution to the work reported, whether that is in the conception, study design, execution, acquisition of data, analysis and interpretation, or in all these areas; took part in drafting, revising or critically reviewing the article; gave final approval of the version to be published; have agreed on the journal to which the article has been submitted; and agree to be accountable for all aspects of the work.

Funding

This study was funded by the National Natural Science Foundation of China (82470192), the Jiangsu Natural Science Foundation (BK20241768), Medical Scientific Research Project of Jiangsu Provincial Health Commission (MQ2025025, Z2024062), Medical Science and Technology Innovation Project of Xuzhou Health Commission (XWKYHT20240109), Science and Technology Development Fund of Affiliated Hospital of Xuzhou Medical University (XYFY202314), and Jiangsu Province High-Level Hospital Construction Project (GSPJS202501).

Disclosure

The authors declare that they have no conflict of interest.

References

1. Sehn LH, Salles G. Diffuse large B-cell lymphoma. *N Engl J Med*. 2021;384(9):842–858. doi:10.1056/NEJMra2027612
2. Coiffier B, Thieblemont C, Van Den Neste E, et al. Long-term outcome of patients in the LNH-98.5 trial, the first randomized study comparing rituximab-CHOP to standard CHOP chemotherapy in DLBCL patients: a study by the Groupe d'Etudes des Lymphomes de l'Adulte. *Blood*. 2010;116(12):2040–2045. doi:10.1182/blood-2010-03-276246
3. Crump M, Neelapu SS, Farooq U, et al. Outcomes in refractory diffuse large B-cell lymphoma: results from the international SCHOLAR-1 study. *Blood*. 2017;130(16):1800–1808. doi:10.1182/blood-2017-03-769620
4. Locke FL, Ghobadi A, Jacobson CA, et al. Long-term safety and activity of axicabtagene ciloleucel in refractory large B-cell lymphoma (ZUMA-1): a single-arm, multicentre, Phase 1–2 trial. *Lancet Oncol*. 2019;20(1):31–42. doi:10.1016/S1470-2045(18)30864-7
5. Hu Y, Li J, Ni F, et al. CAR-T cell therapy-related cytokine release syndrome and therapeutic response is modulated by the gut microbiome in hematologic malignancies. *Nat Commun*. 2022;13(1):5313. doi:10.1038/s41467-022-32960-3
6. Neelapu SS, Tummala S, Kebriaei P, et al. Chimeric antigen receptor T-cell therapy — assessment and management of toxicities. *Nat Rev Clin Oncol*. 2018;15(1):47–62. doi:10.1038/nrclinonc.2017.148
7. Hou K, Wu Z-X, Chen X-Y, et al. Microbiota in health and diseases. *Signal Transduction Targeted Ther*. 2022;7(1):135. doi:10.1038/s41392-022-00974-4
8. Gopalakrishnan V, Helmink BA, Spencer CN, et al. The influence of the gut microbiome on cancer, immunity, and cancer immunotherapy. *Cancer Cell*. 2018;33(4):570–580. doi:10.1016/j.ccell.2018.03.015
9. Diefenbach CS, Peters BA, Li H, et al. Microbial dysbiosis is associated with aggressive histology and adverse clinical outcome in B-cell non-Hodgkin lymphoma. *Blood Adv*. 2021;5(5):1194–1198. doi:10.1182/bloodadvances.2020003129
10. Lin Z, Mao D, Jin C, et al. The gut microbiota correlate with the disease characteristics and immune status of patients with untreated diffuse large B-cell lymphoma. *Front Immunol*. 2023;14:1105293. doi:10.3389/fimmu.2023.1105293
11. Zhang PF, Xie D. Targeting the gut microbiota to enhance the antitumor efficacy and attenuate the toxicity of CAR-T cell therapy: a new hope? *Front Immunol*. 2024;15:1362133. doi:10.3389/fimmu.2024.1362133
12. Bolyen E, Rideout JR, Dillon MR, et al. Reproducible, interactive, scalable and extensible microbiome data science using QIIME 2. *Nat Biotechnol*. 2019;37(8):852–857. doi:10.1038/s41587-019-0209-9
13. Callahan BJ, McMurdie PJ, Rosen MJ, et al. DADA2: high-resolution sample inference from Illumina amplicon data. *Nat Meth*. 2016;13(7):581–583. doi:10.1038/nmeth.3869
14. Segata N, Izard J, Waldron L, et al. Metagenomic biomarker discovery and explanation. *Genome Biol*. 2011;12(6):R60. doi:10.1186/gb-2011-12-6-r60

15. Douglas GM, Maffei VJ, Zaneveld JR, et al. PICRUSt2 for prediction of metagenome functions. *Nat Biotechnol*. 2020;38(6):685–688. doi:10.1038/s41587-020-0548-6
16. Kanehisa M, Goto S. KEGG: kyoto encyclopedia of genes and genomes. *Nucleic Acids Res*. 2000;28(1):27–30. doi:10.1093/nar/28.1.27
17. Parks DH, Tyson GW, Hugenholtz P, et al. STAMP: statistical analysis of taxonomic and functional profiles. *Bioinformatics*. 2014;30(21):3123–3124. doi:10.1093/bioinformatics/btu494
18. Smith M, Dai A, Ghilardi G, et al. Gut microbiome correlates of response and toxicity following anti-CD19 CAR T cell therapy. *Nat Med*. 2022;28(4):713–723. doi:10.1038/s41591-022-01702-9
19. Saha S, Rehman L, Rehman A, et al. Longitudinal analysis of gut microbiome and metabolome correlates of response and toxicity with idecabtagene vicleucel. *Blood Adv*. 2025;9(14):3429–3440. doi:10.1182/bloodadvances.2024014476
20. Di Vincenzo F, Del Gaudio A, Petito V, et al. Gut microbiota, intestinal permeability, and systemic inflammation: a narrative review. *Intern Emerg Med*. 2024;19(2):275–293. doi:10.1007/s11739-023-03374-w
21. Dumitru IG, Todor SB, Ichim C, et al. A literature review on the impact of the gut microbiome on cancer treatment efficacy, disease evolution and toxicity: the implications for hematological malignancies. *J Clin Med*. 2025;14(9):2982. doi:10.3390/jcm14092982
22. Vétizou M, Pitt JM, Daillère R, et al. Anticancer immunotherapy by CTLA-4 blockade relies on the gut microbiota. *Science*. 2015;350(6264):1079–1084. doi:10.1126/science.aad1329
23. Asokan S, Cullin N, Stein-Thoeringer CK, et al. CAR-T cell therapy and the gut microbiota. *Cancers*. 2023;15(3):794. doi:10.3390/cancers15030794
24. Routy B, Le Chatelier E, Derosa L, et al. Gut microbiome influences efficacy of PD-1–based immunotherapy against epithelial tumors. *Science*. 2018;359(6371):91–97. doi:10.1126/science.aan3706
25. Chaput N, Lepage P, Coutzac C, et al. Baseline gut microbiota predicts clinical response and colitis in metastatic melanoma patients treated with ipilimumab. *Ann Oncol*. 2017;28(6):1368–1379. doi:10.1093/annonc/mdx108
26. Matson V, Fessler J, Bao R, et al. The commensal microbiome is associated with anti-PD-1 efficacy in metastatic melanoma patients. *Science*. 2018;359(6371):104–108. doi:10.1126/science.aao3290
27. Zhang M, Liu J, Xia Q. Role of gut microbiome in cancer immunotherapy: from predictive biomarker to therapeutic target. *Exp Hematol Oncol*. 2023;12(1):84. doi:10.1186/s40164-023-00442-x
28. Heshiki Y, Vazquez-Uribe R, Li J, et al. Predictable modulation of cancer treatment outcomes by the gut microbiota. *Microbiome*. 2020;8(1):28. doi:10.1186/s40168-020-00811-2
29. Allison SD, Martiny JBH. Resistance, resilience, and redundancy in microbial communities. *Proc Natl Acad Sci*. 2008;105(supplement_1):11512–-11519. doi:10.1073/pnas.0801925105
30. Li Z, Xiong W, Liang Z, et al. Critical role of the gut microbiota in immune responses and cancer immunotherapy. *J Hematol Oncol*. 2024;17(1):33.
31. Peled JU, Gomes ALC, Devlin SM, et al. Microbiota as predictor of mortality in allogeneic hematopoietic-cell transplantation. *N Engl J Med*. 2020;382(9):822–834. doi:10.1056/NEJMoa1900623
32. Machiels K, Joossens M, Sabino J, et al. A decrease of the butyrate-producing species Roseburia hominis and Faecalibacterium prausnitzii defines dysbiosis in patients with ulcerative colitis. *Gut*. 2014;63(8):1275–1283. doi:10.1136/gutjnl-2013-304833
33. Shay KP, Moreau RF, Smith EJ, et al. Alpha-lipoic acid as a dietary supplement: molecular mechanisms and therapeutic potential. *Biochimica et Biophysica Acta*. 2009;1790(10):1149–1160. doi:10.1016/j.bbagen.2009.07.026
34. Mostafavi Abdolmaleky H, Zhou J-R, Dysbiosis GM. Oxidative stress, inflammation, and epigenetic alterations in metabolic diseases. *Antioxidants*. 2024;13(8):985. doi:10.3390/antiox13080985
35. Yang Y, Xiao Y, Jiang Y, et al. Alpha-lipoic acid promotes intestinal epithelial injury repair by regulating MAPK signaling pathways. *Mediators Inflamm*. 2022;2022(1):1894379. doi:10.1155/2022/1894379